# The Prospect of Reconfigurable Intelligent Surfaces in Integrated Access and Backhaul Networks

Maria Diamanti<sup>®</sup>, *Graduate Student Member, IEEE*, Panagiotis Charatsaris<sup>®</sup>, Eirini Eleni Tsiropoulou<sup>®</sup>, *Senior Member, IEEE*, and Symeon Papavassiliou<sup>®</sup>, *Senior Member, IEEE* 

Abstract—The Integrated Access and Backhaul (IAB) technology provides a new view of the backhauling problem, especially when targeting end-to-end service provisioning. The IAB paradigm - being well aligned with the vision of Unmanned Aerial Vehicles (UAVs) - when combined with the benefits of the Reconfigurable Intelligent Surface (RIS) technology, offers to the future wireless networks the attributes of reconfigurability and energy efficiency. In this paper, we demonstrate the prospect of RIS in an UAV-assisted IAB network targeting energy-efficient operation, while accounting for the transmissions established at both the wireless access and backhaul network parts. We introduce a dynamic resource management framework that targets end-to-end energy efficiency optimization, while considering as controllable parameters the RIS elements' phase shifts, the system bandwidth split between access and backhaul, and the transmission powers of both the UAV and the users. The corresponding joint optimization problem is formulated and treated via a distributed single-leader multiple-followers Stackelberg game-theoretic approach. The adaptation of the proposed framework is, also, demonstrated for the treatment of the IAB network's end-to-end data rate optimization. The framework's performance evaluation highlights the benefits achieved at both the users' and UAV's energy efficiency, by the joint exploitation of UAVs, IAB, and RIS technologies.

Index Terms—Reconfigurable intelligent surfaces, integrated access and backhaul networks, game theory, energy efficiency.

## I. INTRODUCTION

THE NETWORK reconfiguration and adaptability is considered as a prominent network paradigm and is expected to play a significant role in elevating future network performance and increasing efficiency. The integration of advanced hardware and software technologies and components into wireless systems, has opened a new horizon to meet the capacity and coverage requirements of future wireless

Manuscript received May 31, 2021; revised August 25, 2021; accepted November 2, 2021. Date of publication November 9, 2021; date of current version May 20, 2022. This work was supported by the Hellenic Foundation for Research and Innovation (H.F.R.I.) through the "1st Call for H.F.R.I. Research Projects to support Faculty members and Researchers and the Procurement of High-Cost Research Equipment Grant" under Project HFRI-FM17-2436. The work of Eirini Eleni Tsiropoulou was supported by NSF under Grant CRII-1849739. (Corresponding author: Eirini Eleni Tsiropoulou.)

Maria Diamanti, Panagiotis Charatsaris, and Symeon Papavassiliou are with the School of Electrical and Computer Engineering, National Technical University of Athens, 157 80 Athens, Greece (e-mail: mdiamanti@netmode.ntua.gr; el16024@mail.ntua.gr; papavass@mail.ntua.gr).

Eirini Eleni Tsiropoulou is with the Department of Electrical and Computer Engineering, University of New Mexico, Albuquerque, NM 87131 USA (e-mail: eirini@unm.edu).

Digital Object Identifier 10.1109/TGCN.2021.3126784

networks, along with the satisfaction of the users' elevated needs. For instance, Unmanned Aerial Vehicles (UAVs) are anticipated to revolutionize the way that wireless communications are performed. By providing communication services on-demand, the UAVs contribute to the maintenance of the network's sustainability in cases that the underlying network infrastructure is proven to be limited. Recently, the efforts of the research community and the standardization bodies have unveiled several opportunities, enabled by emerging technologies, which will gradually result to the maturity of the UAV-assisted communications. Characteristic example of such a technology is the Integrated Access and Backhaul (IAB) network deployment [1].

In particular, this paradigm proposes that the Next Generation Node Bases (gNBs), referred to as IAB nodes, wirelessly relay the mobile traffic in a multi-hop manner to finally reach the IAB donor, which is connected to the core Internet with fiber infrastructure [2]. Within the aforementioned context, by increasing the UAV's (acting as an IAB node) degrees of freedom in terms of wireless service provisioning and its connectivity to the core network, the IAB network architecture is seen as one of the primary enablers of the vision of fully reconfigurable and energy-efficient wireless networks.

Building on the concept and potentials of the IAB networks, another interesting technology that has lately received notable attention and is deeply related to the future wireless networks' attributes of reconfigurability and energy efficiency, is the so-called Reconfigurable Intelligent Surface (RIS). Constructed by engineered meta-materials, which usually serve as reflectors, RIS allows for the software-based control of the reflected signals' electromagnetic properties [3]. Hence, by appropriately manipulating the reflected signals, RIS is expected to improve the overall received signal strength and ameliorate the communications' energy efficiency. Some initial real experiments in indoor and outdoor environments have already shown the great energy saving and data rate improvement enabled by the RIS technology [4].

In this paper, we capitalize on the joint benefits of IAB and RIS, and we design and propose an end-to-end resource management framework, tailored to the converged RIS-aided and UAV-assisted network deployments. Such a converged network deployment is adapted to the future urban UAV-assisted communications, in which the wireless propagation environment can be appropriately controlled to account for different objectives, while the UAVs serve as integral part of the network's infrastructure to provide end-to-end connectivity under adverse

2473-2400 © 2021 IEEE. Personal use is permitted, but republication/redistribution requires IEEE permission. See https://www.ieee.org/publications/rights/index.html for more information.

situations. In this context, we consider the uplink communications and treat the distinct objective of end-to-end energy efficiency maximization, via our proposed dynamic and fully reconfigurable resource management framework. Complementary to this, and for better revealing the benefits and tradeoffs of the obtained solution when aiming at energy efficiency, we also analyze and evaluate the application of the proposed framework, under a different optimization objective, namely the end-to-end data rate optimization. Towards the realization of each one of the aforementioned objectives, we jointly treat and dynamically optimize the RIS elements' phase shifts, the bandwidth splitting between the wireless access and backhaul parts of the network, as well as the users' and the serving UAV's transmission powers.

The proposed framework promotes the reconfigurability, programmability and adaptability of the wireless network, not only by partially controlling the radio propagation conditions, but also from the dynamic resource management perspective. With respect to the former, a smart radio environment is created, where the wireless propagation conditions are co-engineered with the physical-layer signaling, while we investigate how to utilize this new capability for improved energy-efficient network design. With respect to the latter, the system bandwidth and transmission powers are becoming controllable parameters, which are intelligently and dynamically adjusted, towards meeting specific user and system objectives.

#### A. Related Work

Although the paradigm of IAB deployment is still at its initial stages, there exist research works in the literature that deal with timely resource allocation problems under the umbrella of IAB. In [5], a multi-hop IAB network that operates under the combination of Time (TDMA) and Frequency Division Multiple Access (FDMA) is considered, to coordinate the transmissions along the different wireless links. The problem of subchannel and power allocation is formulated to maximize the sum system throughput, while insights regarding the optimal IAB node placement and user association are presented. Under a similar multi-IAB-node, though singlehop, network topology, the authors in [6] treat the problem of spectrum assignment to the different IAB nodes via a deep reinforcement learning approach, while trying to maximize the sum users' throughput. Also, a joint traffic load balancing and interference mitigation optimization model is introduced in [7], targeting at the maximization of the overall network's capacity. The joint optimization problem is organized in two subproblems, which are solved iteratively following the successive convex approximation method.

Moving from the terrestrial network deployments to the promising inclusion of the UAVs within the concept of IAB, different challenges and considerations behind the idea of UAV-based communications in Millimeter Wave (mmWave) frequencies are discussed in [8], while investigating the effect of UAVs' and users' mobility to the network's performance. Other works that deal with backhaul-aware UAV-assisted networks can be found in [9], [10]. In the former, the joint problem of 3D UAV positioning, wireless backhaul sub-band

assignment and downlink transmission power allocation is formulated, such that the UAV's transmission power is minimized, while accounting for the users' Quality of Service (QoS) prerequisites. On the other hand, the uplink communication is assumed in [10] and the joint user association, power and bandwidth assignment is determined to maximize the sum system throughput. Targeting at the interference mitigation at the access and backhaul links, the authors in [11] introduce a joint optimization problem of the users' association to the base stations, the downlink power allocation regarding the access and backhaul transmissions, and the UAV's deployment within the examined communications environment.

To further enhance the energy and spectral efficiency of 5G and beyond networks, significant attention has been paid to the incorporation of the RIS under a plethora of different communication scenarios. Initial works, such as [12], [13], focused on simple use cases and scrutinized the joint problems of power control and RIS elements' phase shifts optimization. Both aforementioned works compared the performance gain incurred by the RIS considering different multiple access techniques, such as orthogonal and non-orthogonal, while targeting at the users' power minimization and data rate maximization, respectively. Similar problems have been formulated for more complex setups, such as the Multiple-Input Single-Output (MISO) Non-Orthogonal Multiple Access (NOMA) network considered in [14]. In this work, the authors addressed the sum users' data rate maximization problem under a combination of machine learning algorithms, based on K-means Gaussian Mixture Model (K-GMM) and deep Q-network (DQN), while optimizing the RIS's passive beamforming vector, and the users' decoding order and power allocation, subject to their data rate prerequisites.

Most of the relevant existing research works, exclusively consider the downlink direction of the RIS-enabled communications, while only a few attempts have been made towards modeling and optimizing the wireless network's resources treating the uplink direction. Focusing on the uplink communication of a RIS-enabled wireless cellular network, the authors in [15] deal with the maximization problem of the sum rate of all users subject to their individual power constraints. In [16], a comparative study between the non-orthogonal multiple access (NOMA) and orthogonal multiple access (OMA) RISenabled networks is presented, examining both the uplink and downlink communication for several fading characteristics of the communications environment. The authors conclude that the RIS-enabled network consistently achieves high signal-tonoise ratio, while its increasing trend is not affected by the number of RIS elements and/or the fading parameters. Also, in [17], the tradeoff between the energy and spectral efficiency in the uplink communication is studied by jointly optimizing the users' transmit precoding and the RIS's reflective beamforming to maximize the resource efficiency.

Finally, the joint power of RIS and UAV-assisted communications has been also examined. In [18], the deployment of a RIS on the boundary of a UAV's serving area is considered and the joint users' resource allocation and UAV's trajectory optimization is designed to take advantage by the existence of the RIS. The authors in [19] introduce a machine

learning approach to jointly determine the UAV's trajectory, the phase shifts of the RIS elements, the power allocation policy from the UAV to the users, and the dynamic decoding order, towards minimizing the overall system's energy consumption. The scenario of a RIS mounted on an UAV to maintain the Line-of-Sight (LoS) communication is studied in [20], and similarly a joint resource allocation and UAV mobility problem is devised.

#### B. Contributions & Outline

Undoubtedly, the existing research has focused on different network optimization problems pertaining to the emerging technologies of UAVs, IAB and RIS, and has identified their challenges and performance gains in a rather fragmented manner. To the best of our knowledge, there exists no work in the current literature that identifies the prospect of RIS and its added value in a backhaul-aware network optimization process, as the one revealed by the IAB paradigm. Considering at the same time both the access and backhauling requirements and resource allocation, is of paramount practical importance, to exploit the benefits of the aforementioned technological advances at their full capacity.

In this paper, our objective is to exactly address this issue and demonstrate the prospect of RIS in an UAV-assisted IAB network targeting its energy efficiency. In this way, we aim at introducing a dynamic, intelligent, and reconfigurable resource optimization framework, which jointly accounts for the access and backhaul resource optimization and operation, towards ensuring the end-to-end service provisioning for the users. Respecting the need for the design and deployment of decentralized resource management processes, we capitalize on the distributed nature of game theory and Stackelberg games, and accordingly we jointly treat the wireless propagation environment's adaptation and the network's resources' optimization under a low-complexity end-to-end framework. It is shown that the use of RIS can provide significant improvements in terms of higher sum users' energy efficiency, driving the overall equilibrium and the UAV's performance at more energy-efficient points. The specific key contributions of this paper are summarized as follows:

- A system model capturing a RIS-aided and UAV-assisted IAB network is introduced, accounting for the communications established at the uplink of both the wireless access and wireless backhaul network parts (Section II).
- 2) The problem of the IAB network's end-to-end resource management towards its energy efficiency optimization, is formulated and treated via a distributed Stackelberg game-theoretic approach. The proposed approach comprises of three stages, across which the following parameters are controlled and dynamically optimized: a) the RIS elements' phase shifts, b) the bandwidth splitting among the wireless access and backhaul network parts, and c) the users' and d) the UAV's uplink transmission powers (Section III).
- 3) The UAV, acting as leader, determines in the first stage the RIS elements' phase shifts that maximize the sum users' signal strength in the uplink, following

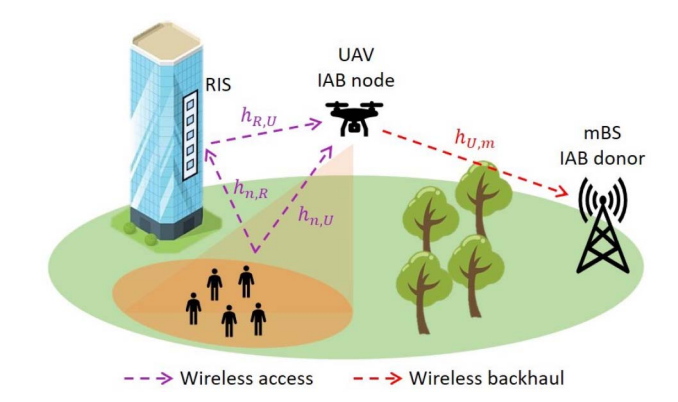


Fig. 1. Overview of the RIS-aided and UAV-assisted Integrated Access and Backhaul (IAB) network.

- a low-complexity heuristic approach (Section III-B). Then, the UAV calculates the bandwidth splitting and its uplink transmission power to the IAB donor (Section III-C). In the third stage, the users, i.e., the followers, optimize their uplink transmission powers to the UAV in a distributed manner (Section III-D). The overall Stackelberg game-based algorithm is presented in Section III-E.
- 4) The applicability and adaptation of the proposed resource management framework is, also, demonstrated for the treatment of the IAB network's end-to-end data rate optimization problem. The solution is obtained following a similar distributed Stackelberg game-theoretic approach with its energy efficiency-related counterpart (Section IV). This alternative optimization objective serves, also, as the basis for highlighting the benefits and tradeoffs of the obtained solution when aiming at energy efficiency.
- 5) The overall network's performance is evaluated and indicative numerical results are presented that demonstrate the benefits introduced at both the users' and UAV's energy efficiency, by the joint exploitation of UAV, IAB and RIS technologies (Section V).

Notation Conventions: The notations used in the remainder of the paper are listed as follows. The vectors and matrices are denoted by bold-face letters and are accompanied by their size.  $\mathbb{C}^{X\times Y}$  represents the  $X\times Y$  space of a complex-valued matrix. Given any matrix  $\mathbf{G}$ ,  $\mathbf{G}^T$  and  $\mathbf{G}^H$  indicate the transpose and conjugate transpose of the general matrix  $\mathbf{G}$ , accordingly, while  $G_{i,j}$  is the (i,j)-th element of the matrix. Given any vector  $\mathbf{g}$ ,  $diag(\mathbf{g})$  refers to the diagonal matrix, whose elements on the main diagonal are the elements of the vector  $\mathbf{g}$ .  $\mathcal{CN}(\mu,\sigma^2)$  denotes the Circularly Symmetric Complex Gaussian (CSCG) distribution with mean  $\mu$  and variance  $\sigma^2$ , and  $\sim$  stands for "distributed as". Considering a complex number g, |g| denotes its absolute value and  $\angle g$  its phase. Considering any function f, dom denotes the domain of the function f.

## II. SYSTEM MODEL

We consider the uplink communication of a RIS-aided and UAV-assisted two-tier IAB network, as illustrated in Fig. 1,

consisting of |N| users, with  $N = \{1, \dots, n, \dots, |N|\}$  denoting their set, a UAV and a micro Base Station (mBS). The UAV, serving as an IAB node, collects the users' data in the first tier and in the second tier, forwards this data to the mBS (i.e., the IAB donor) through the wireless backhaul. In this paper, the position of the UAV is considered to be fixed throughout the operation of the resource management procedure. It should be noted that the problem of the UAV's trajectory optimization and its impact on the resource management under different operation scenarios and requirements, though interesting and challenging by itself, is considered beyond the scope of this paper and is part of our current and future work. All the involved transmitting/receiving entities, i.e., the users, the UAV, and the mBS, bear single-antenna transmitters and receivers. The IAB network operates in out-of-band mode, meaning that the wireless access and backhaul links use different frequency bands. Hence, the total system bandwidth W [Hz] is split into two parts  $\mu W$  and  $(1 - \mu) W$  [Hz] to facilitate the wireless access and backhaul communications. respectively, where  $\mu \in [0,1]$  is the corresponding bandwidth splitting ratio. The users' transmissions in the first tier are multiplexed using the combination of power-domain NOMA and Successive Interference Cancellation (SIC) techniques.

# A. Path Loss Model

In the considered IAB network, the path loss between any network entity and the UAV is stochastically determined to account for both the Line-of-Sight (LoS) and non LoS (NLoS) cases [10]. The probability that the wireless link between a network entity and the UAV is LoS derives from the function:

$$Pr^{LoS}(z_U, d) = \frac{1}{1 + \psi e^{-\beta(\theta - \psi)}},$$
 (1)

where  $\theta = \frac{180}{\pi} sin^{-1}(\frac{z_U}{d})$  [rad] is the elevation angle between the network entity and the UAV, with d [m] denoting their in-between Euclidean distance and  $z_U$  [m] representing the UAV's altitude. Also,  $\psi, \beta \in \mathbb{R}^+$  are constants depending on the carrier frequency and the type of the communications environment, e.g., rural, urban, suburban. The path loss for the LoS case between a network entity and the UAV is defined as a function of their in-between Euclidean distance d as:

$$PL^{LoS}(d) = \eta_{LoS} \left(\frac{4\pi f_c d}{c}\right)^{a_U},\tag{2}$$

while the respective path loss model for the NLoS case is:

$$PL^{NLoS}(d) = \eta_{NLoS} \left(\frac{4\pi f_c d}{c}\right)^{a_U},$$
 (3)

where  $f_c$  [Hz] is the carrier frequency, c [m/s] is the speed of light,  $a_U$  is the path loss exponent and  $\eta_{LoS}, \eta_{NLoS}$  [dB] are the excessive path loss coefficients, such that  $\eta_{NLoS} > \eta_{LoS} > 1$ . The overall expected path loss is probabilistically given by:

$$\overline{PL}(z_U, d) = Pr^{LoS}PL^{LoS} + (1 - Pr^{LoS})PL^{NLoS}.$$
 (4)

Focusing on the first network tier, the prospect of RIS is scrutinized and a Uniform Linear Array (ULA) consisting of a

set of  $M=\{1,\ldots,m,\ldots,|M|\}$  reflecting elements is considered, placed at a height of  $z_R$  [m] above the ground. For each reflecting element m of the RIS, we denote as  $\omega_m \in [0,2\pi)$  the phase shift of the reflection and we assume that no change in the amplitude of the incident signal is incurred, i.e., the amplitude of the reflection coefficient is equal to 1. The diagonal reflection matrix of the RIS elements is noted as  $\Omega=diag(e^{j\omega_1},\ldots,e^{j\omega_{|M|}})\in \mathbb{C}^{|M|\times|M|},$  while the first RIS element is used as a reference point for the performance of the subsequent calculations. The direct communication link between a user n and the UAV follows the probabilistic path loss modeling, such that  $PL_{n,U}=\overline{PL}(z_U,d_{n,U}),$  where  $d_{n,U}$  [m] is the Euclidean distance between user n and the UAV. Thus, the corresponding channel gain coefficient  $h_{n,U}\in\mathbb{C}$  is given as follows:

$$h_{n,U} = \sqrt{\frac{1}{PL_{n,U}}}\tilde{h},\tag{5}$$

with  $\tilde{h} \backsim \mathcal{CN}(0,1)$  denoting the random scattering component captured by a zero-mean and unit-variance complex Gaussian random variable. The path loss between a user n and the RIS is  $PL_{n,R} = \rho(d_{n,R})^{a_R}$ , where  $\rho$  [dB] is the path loss at the reference distance 1m,  $d_{n,R}$  [m] is the Euclidean distance between user n and the reference point of RIS and  $a_R$  is the path loss exponent [21]. Assuming that the RIS is in the users' proximity, the channel gain coefficient  $\mathbf{h}_{n,R} \in \mathbb{C}^{|M| \times 1}$  between a user n and the RIS is:

$$\mathbf{h}_{n,R} = \sqrt{\frac{1}{PL_{n,R}}} \left[ 1, e^{-j\frac{2\pi}{\lambda}d_s\phi_{n,R}}, \dots, e^{-j\frac{2\pi}{\lambda}(|M|-1)d_s\phi_{n,R}} \right]^T,$$
(6)

where  $\lambda$  [m] is the carrier wavelength,  $d_s$  [m] is the antenna separation and  $\phi_{n,R}$  is the cosine of the angle of arrival of the user's signal to the RIS. The channel gain  $\mathbf{h}_{R,U} \in \mathbb{C}^{|M| \times 1}$  of the RIS-to-UAV wireless link is modeled as:

$$\mathbf{h}_{R,U} = \sqrt{\frac{1}{PL_{R,U}}} \left( \sqrt{\frac{\kappa}{1+\kappa}} \mathbf{h}_{R,U}^{LoS} + \sqrt{\frac{1}{1+\kappa}} \mathbf{h}_{R,U}^{NLoS} \right), \quad (7)$$

where  $PL_{R,U} = \overline{PL}(z_U - z_R, d_{R,U})$  is the link's path loss determined probabilistically and  $\kappa$  is the Rician factor. Also,  $\mathbf{h}_{R,U}^{LoS} = [1, e^{-j\frac{2\pi}{\lambda}ds\phi_{R,U}}, \dots, e^{-j\frac{2\pi}{\lambda}(|M|-1)ds\phi_{R,U}}]^T$  is the LoS component, with  $\phi_{R,U}$  denoting the cosine of the angle of departure of the signal from the RIS to the UAV, and  $\mathbf{h}_{R,U}^{NLoS} \backsim \mathcal{CN}(0,1)$  is the NLoS component, which follows the complex Gaussian distribution. Subsequently, the total channel power gain between a user n and the UAV is given by:

$$G_n = \left| h_{n,U} + \mathbf{h}_{R,U}^H \mathbf{\Omega} \mathbf{h}_{n,R} \right|^2. \tag{8}$$

With reference to the second IAB network tier, the path loss of the wireless backhaul link between the UAV and the mBS follows the probabilistic model and is defined as  $PL_{U,m} = \overline{PL}(z_U, d_{U,m})$ , where  $d_{U,m}$  [m] is the Euclidean distance between the UAV and the mBS. The channel gain coefficient  $h_{U,m} \in \mathbb{C}$  between the UAV and the mBS is:

$$h_{U,m} = \sqrt{\frac{1}{PL_{U,m}}}\tilde{h}',\tag{9}$$

with  $\tilde{h'} \backsim \mathcal{CN}(0,1)$  accounting for the random scattering, while the respective channel power gain is noted as:

$$G_U = \left| h_{U,m} \right|^2. \tag{10}$$

## B. Communications Model

Focusing on the communication between the users and the UAV, the SIC technique is implemented at the UAV's receiver to decode the received signals. Without loss of generality, we assume that the users' total channel gains  $G_n$  are sorted as  $G_1 \leq \cdots \leq G_n \leq \cdots \leq G_{|N|}$  and decoding starts from the highest channel gain user. Thus, a user's n achieved data rate through the wireless access  $(R_n^{AC})$  is as follows:

$$R_n^{AC} = \mu W \log_2 \left( 1 + \frac{G_n P_n}{\sum_{n'=1}^{n-1} G_{n'} P_{n'} + \mu W N_0} \right) [bps], (11)$$

where  $P_n$  [W] denotes the uplink transmission power of user n and  $N_0$  [dBm/Hz] is the power spectral density of the zero-mean Additive White Gaussian Noise (AWGN).

Let  $P_U$  [W] indicate the UAV's transmission power for forwarding the users' data to the mBS, then the UAV's achieved data rate through the wireless backhaul ( $R_U^{BH}$ ) is:

$$R_U^{BH} = (1 - \mu) W \log_2 \left( 1 + \frac{G_U P_U}{(1 - \mu) W N_0} \right) [bps].$$
 (12)

From the cumulative UAV's achieved data rate  $R_U^{BH}$ , we adopt a proportionally fair approach and derive each user's n achieved data rate at the wireless backhaul  $(R_n^{BH})$  as follows:

$$R_n^{BH} = \frac{R_n^{AC}}{\sum_{n=1}^{|N|} R_n^{AC}} R_U^{BH}[bps]. \tag{13}$$

Accordingly, the user's n end-to-end achieved data rate  $(R_n^{E2E})$  is obtained by:

$$R_n^{E2E} = \min\left(R_n^{AC}, R_n^{BH}\right) [bps]. \tag{14}$$

# III. END-TO-END ENERGY EFFICIENCY OPTIMIZATION

# A. Design for Reconfigurability and Efficiency

In the following, we elaborate on our proposed dynamic and reconfigurable resource management framework that targets the end-to-end energy efficiency optimization of the network topology under consideration. In particular, we seek to dynamically allocate the available spectrum and power resources in both the wireless access and wireless backhaul parts of the considered RIS-aided and UAV-assisted IAB network, while maximizing the overall IAB network's energy efficiency. Under this scope, the corresponding joint optimization problem is formulated, simultaneously accounting for and controlling: a) the RIS elements' phase shifts  $\omega$ , b) the bandwidth splitting ratio parameter  $\mu$ , c) the users' transmission power vector **P** to the UAV, and d) the UAV's transmission power  $P_{II}$  to the mBS. This joint optimization problem is formulated as a single-leader multiple-followers Stackelberg game and treated in three sequential stages. The UAV, acting as the leader, determines in the first stage the optimal RIS elements' phase shifts that enhance its overall received signal strength

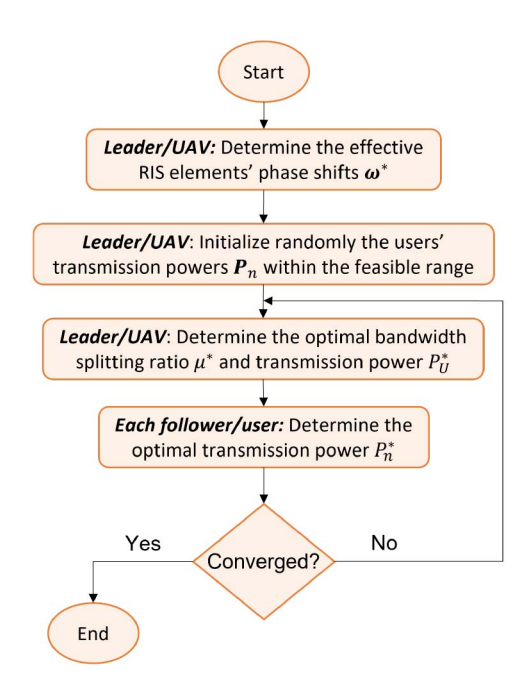


Fig. 2. End-to-end resource management framework overview.

and broadcasts the appropriate control signals to the controller of the RIS. Then, in the second stage, the UAV calculates the bandwidth splitting ratio and its transmission power to the mBS that maximize its energy efficiency. The results of the second stage are fed back to the users, who are acting as the followers, and determine in a distributed and autonomous manner their uplink transmission powers towards maximizing their energy efficiency. The second and third stage of the devised Stackelberg game are played iteratively to converge to the Stackelberg equilibrium. An overview of the proposed end-to-end resource management framework is illustrated in Fig. 2, in the form of a block diagram.

It is noted that in our introduced paradigm and resource management framework, the radio propagation environment, from simply being a passive exogenous entity, it becomes a controllable and reconfigurable element with programmable properties, through the intelligent RIS's phase shifts' adaptation. In this way, the quality of the received signal strength is improved, combating the unfavorable propagation conditions due to the wireless channels' fading, while resulting in reduced transmission powers and interference. As a result, the inclusion of the RIS in the wireless environment provides an extra degree of freedom apart from the typical power and bandwidth control, when seeking to maximize the end-to-end energy efficiency or data rate. Moreover, owing to the emergence of RISs and the advanced intelligent decision-making methods adopted, we treat the wireless environment and resources as part of the overall network design that can be adapted to satisfy specific system and user requirements in a dynamic manner (i.e., dynamic access and backhaul bandwidth splitting).

# B. RIS Elements' Phase Shifts' Adaptation

As discussed earlier, the optimization of the wireless propagation environment, via the constructive beams created by

reflection from the RIS, is used to assist and boost the network's resources' optimization procedure. To achieve this, the UAV determines the effective RIS elements' phase shifts  $\pmb{\omega}^* = [\omega_1, \dots, \omega_m, \dots, \omega_{|M|}]$  that enhance its overall received signal strength, towards further supporting the system's energy efficiency optimization via the optimal bandwidth splitting ratio  $\mu^*$  and its optimal transmission power  $P_{II}^*$  to the mBS. In order for the UAV to maximize the overall received signal strength, it suffices to find the effective RIS elements' phase shifts  $\omega^*$  that maximize the overall channel power gain of the users. Hence, the UAV treats the following optimization problem:

$$\max_{\boldsymbol{\omega}} \sum_{n=1}^{|N|} \left| h_{n,U} + \mathbf{h}_{R,U}^{H} \mathbf{\Omega} \mathbf{h}_{n,R} \right|^{2}$$
 (15a)

s.t. 
$$0 \le \omega_m < 2\pi, \ \forall m \in M.$$
 (15b)

To easier handle the problem in Eq. (15a)-(15b), we denote as  $v_m = e^{j\omega_m}, \forall m \in M$  and define the corresponding  $\text{reflection-coefficient vector } \mathbf{v} \ = \ [v_1, \dots, v_m, \dots, v_{|M|}] \ \in$  $\mathbb{C}^{|M|\times 1}$ . Then, by substituting  $\hat{\mathbf{h}}_{n,R}^H = \mathbf{h}_{R,U}^H diag(\hat{\mathbf{h}}_{n,R}) \in$  $\mathbb{C}^{1\times |M|}$ , the problem in Eq. (15a)-(15b) is equivalently rewritten as:

$$\max_{\mathbf{v}} \sum_{n=1}^{|N|} \left| h_{n,U} + \hat{\mathbf{h}}_{n,R}^H \mathbf{v} \right|^2$$
 (16a)

s.t. 
$$|v_m| = 1, \ \forall m \in M,$$
 (16b)

where Eq. (16b) is the unit-modulus equivalent constraint to the one expressed in Eq. (15b). Eq. (16a) is a non-concave function with respect to the vector v and the unit-modulus constraint in Eq. (16b) defines, also, a non-convex set. Thus, the optimization problem in Eq. (16a)-(16b) is generally nonconcave and there exists no standard method to derive a globally optimal solution [21], [22]. For this reason, we adopt an effective and of low-complexity heuristic approach [12], as presented in the sequel.

Consider the case when a single user, denoted by n = 1, exists in the system. Then, it generally holds true that this user's channel power gain is maximized when its signals arriving from different paths at the receiver of the UAV, i.e., the direct signal and the signal created by reflection from the RIS, are perfectly aligned and coherently combined [12], [23]. This happens when the phase shifts of the direct and the reflected signals are equal, such as:

$$\angle h_{1,U} = -\angle \hat{\mathbf{h}}_{1,R} + \angle \mathbf{v} \Leftrightarrow \angle \mathbf{v} = \angle h_{1,U} + \angle \hat{\mathbf{h}}_{1,R},$$
 (17)

concluding to the optimal  $1 \times |M|$  phase-shift vector  $\boldsymbol{\omega}^* = \angle \mathbf{v}$ for the single-user system.

As a logical consequence of Eq. (17), in the multiple-user case, there exists a different reflection-coefficient vector  $\mathbf{v}_n =$  $[v_{n,1},\ldots,v_{n,m},\ldots,v_{n,|M|}]\in\mathbb{C}^{|M|\times 1}$  for each user n that maximizes each individual user's n channel power gain, which is given by:

$$\mathbf{v}_n = e^{j \angle h_{n,U}} e^{j \angle \hat{\mathbf{h}}_{n,R}}, \ \forall n \in N.$$
 (18)

Apparently, the reflection-coefficient vectors  $\mathbf{v}_n$  of different users differ between each other, which suggests that there does not exist a single reflection-coefficient vector v maximizing all users' |N| channel power gains concurrently.

Towards striking a balance between the different users' reflection-coefficient vectors  $\mathbf{v}_n$  and obtaining a global solution for the RIS elements' phase shifts' adaptation problem, we introduce for each user n an appropriate weight factor  $w_n \in [0,1]$  and derive the linear combination of the overall users' reflection-coefficients  $\mathbf{v}_n$  as follows:

$$\mathbf{v} = \sum_{n=1}^{|N|} w_n \mathbf{v}_n,\tag{19}$$

such that it holds true that  $\sum_{n=1}^{|N|} w_n = 1$ .

Our ultimate objective is to determine the optimal value of the weight factor  $w_n$  of each term of the reflection-coefficient vector v in Eq. (19) that concludes to an increased sum of the users' channel power gains, as imposed by Eq. (16a). Thus, the corresponding optimization problem to be addressed to derive an efficient and effective RIS elements' phase shifts' adaptation is formulated as:

$$\max_{\mathbf{w}} \sum_{n=1}^{|N|} \left| h_{n,U} + \mathbf{h}_{R,U}^{H} \mathbf{\Omega} \mathbf{h}_{n,R} \right|^{2}$$
 (20a)

$$s.t. 0 \le w_n \le 1, \forall n \in N$$
(20b)

$$\sum_{n=1}^{|N|} w_n = 1 \tag{20c}$$

where the reflection matrix  $\Omega$  is calculated with backward induction as  $\Omega = diag(e^{j \angle \mathbf{v}})$ . Also, w  $[w_1,\ldots,w_n,\ldots,w_{|N|}]$  is the vector of the users' assigned weight factors. The optimization problem defined in Eq. (20a)-(20c) comprises from a non-negative linear objective function and constraints, which can be optimized in a straightforward manner to conclude to the optimal weights  $\mathbf{w}^*$ .

The optimal weights' w\* derivation leads to a single and effective RIS elements' reflection-coefficient vector  $\mathbf{v}^* =$  $[v_1,\ldots,v_m,\ldots,v_{|M|}]$ , and eventually determines the effective RIS elements' phase shifts  $\boldsymbol{\omega}^* = [\omega_1, \dots, \omega_m, \dots, \omega_{|M|}].$ 

# C. Leader's Energy Efficiency Optimization

Following the RIS elements' phase-shift adaptation, the UAV playing the role of the leader, derives the optimal bandwidth splitting ratio  $\mu^*$  and its optimal transmission power  $P_{II}^*$ to the mBS, given the users' uplink transmission power vector  $\mathbf{P} = [P_1, \dots, P_n, \dots, P_{|N|}],$  towards maximizing its energy efficiency  $EE_U$ . The corresponding optimization problem, solved by the leader, is formulated as follows:

$$\max_{\substack{\mu, P_U \\ \text{s.t. } 0 \leq \mu \leq 1}} EE_U(\mu, P_U) = \frac{\sum_{n=1}^{|N|} R_n^{AC} + R_U^{BH}}{P_U}$$
 (21a)

s.t. 
$$0 \le \mu \le 1$$
 (21b)

$$P_U \le P_U^{max} \tag{21c}$$

$$R_n^{E2E} \ge R_{min}, \forall n \in N. \tag{21d}$$

Having the ability to control the network parameters that pertain to both the access and the backhaul network parts, the UAV pursues the maximization of the total achieved data rates at the access and the backhaul network (Eq. (21a)), while trying to minimize its transmission power to the mBS. Eq. (21b) refers to the feasible range of values of the bandwidth splitting ratio parameter  $\mu$ . Also, Eq. (21c) guarantees that the UAV's optimal transmission power to the mBS does not exceed the UAV's maximum power budget  $P_U^{max}$ , while Eq. (21d) reassures that the optimal bandwidth splitting ratio satisfies the users' end-to-end achieved data rate QoS requirement  $R_{min}$ .

The outcome of the optimization problem described in Eq. (21a)-(21d) is the optimal bandwidth splitting ratio  $\mu^*$ and the UAV's optimal transmission power  $P_{II}^*$  to the mBS. To establish the existence of an optimal solution  $(\mu^*, P_I^*)$ for the specific problem, we observe that the numerator of  $EE_U(\mu,P_U)$  consists of two terms, i.e.,  $\sum_{n=1}^{|N|}R_n^{AC}$  and  $R_U^{BH}$ . However, based on Eq. 11 and Eq. 12 and by calculating their derivatives with respect to the bandwidth splitting ratio parameter  $\mu$ , it is concluded that the numerator of  $EE_U(\mu, P_U)$  in Eq. (21a) is not always a concave function on  $\mu$ , complicating twice the derivation of an optimal solution for the two-variable optimization problem in Eq. (21a)-(21d) [24]. To address this problem and provide a tractable solution, we decompose the optimization problem presented in Eq. (21a)-(21d) into an exhaustive search of the optimal value of  $\mu$  over its strategy space, and an optimization problem with respect to the optimal value of  $P_{II}$ . The optimization problem in Eq. (21a)-(21d) is solved with respect to  $P_U$  over different values of the parameter  $\mu$  and ultimately, the values of  $\mu$  and  $P_U$  that yield the maximum energy efficiency, based on Eq. (21a), are selected to serve as the optimal solution  $(\mu^*, P_{II}^*)$ . For all practical purposes, the partitioning of the bandwidth is typically performed into a finite discrete region (i.e., resource blocks or slices of predefined sizes), and therefore the  $\mu$  takes discrete values in a finite strategy space. Thus, for demonstration purposes, we can consider some indicative discrete values of  $\mu$ , e.g.,  $\mu = 0.05, 0.1, 0.15, \dots, 0.95$ , and we determine the corresponding optimal values of  $P_U^*$ , as follows.

Lemma 1: The energy efficiency function  $EE_U$  in Eq. (21a) is strictly quasi-concave with respect to  $P_U$ .

*Proof:* As defined in [25], a function  $f : \mathbb{R}^n \to \mathbb{R}$  is strictly quasi-concave if its sublevel set  $S_a = \{\mathbf{x} | \mathbf{x} \in domf, f(\mathbf{x}) \geq a\}$  is strictly convex for every a, where  $\mathbf{x}$  is the corresponding vector of variables. Accordingly, the sublevel set  $S_a$  defined for the  $EE_U$  function in Eq. (21a) is:

$$S_a = \left\{ P_U | P_U \in domEE_U, \frac{g(P_U)}{P_U} \ge a \right\}, \qquad (22)$$

where  $g(P_U) = \sum_{n=1}^{|N|} R_n^{AC} + R_U^{BH}$  is the sum data rate function, for which it holds true that it is strictly concave on  $P_U$ , since the term  $\sum_{n=1}^{|N|} R_n^{AC}$  is independent of  $P_U$ , and the term  $R_U^{BH}$  is a concave function with respect to  $P_U$ . As a result, when  $a \leq 0$ , then  $S_a$  is obviously convex on  $P_U$ . In the case when a > 0, then the sublevel set in Eq. (22) is rewritten as:

$$S_a = \{ P_U | P_U \in domEE_U, aP_U - g(P_U) \le 0 \}.$$
 (23)

Given that the sum rate function  $g(P_U)$  is strictly concave with respect to  $P_U$ , it follows that  $-g(P_U)$  is strictly convex

on  $P_U$ , while the term  $aP_U$  increases linearly with  $P_U$ . As a result, the sublevel set  $S_a$  in Eq. (22) constitutes a strictly convex set. This completes the proof that the  $EE_U(P_U)$  function is quasi-concave.

Lemma 2: The constraints in Eq. (21b)-(21d) form a compact, i.e., closed and bounded, and convex set.

*Proof:* The constraint in Eq. (21b) generally forms a compact set, while for the rest of the constraints in Eq. (21c)-(21d) we consider the following functions:

$$s_n^{(1)} = P_U - P_U^{max}$$
  

$$s_n^{(2)} = R_{min} - R_n^{E2E}, \forall n \in \mathbb{N}.$$
 (24)

It can be easily proved that the functions  $s^{(1)}$  and  $s_n^{(2)}$ ,  $\forall n \in \mathbb{N}$  are convex on  $P_U$ . Hence, their level sets, defined generally as follows:

$$S_0 = \{ \mathbf{x} | \mathbf{x} \in domf, f(\mathbf{x}) = 0 \}, \tag{25}$$

considering any function f and any vector of variables  $\mathbf{x}$ , are convex sets. This completes the proof.

Based on Lemmas 1-2 and the preceding analysis, the optimization problem defined in Eq. (21a)-(21d) forms a quasiconcave program that belongs in the broader area of concave fractional programming and thus, admits an optimal solution  $P_U^*$  [26]. The solution can be obtained by appropriately transforming the quasi-concave problem into a series of concave problems via existing methods [25], and subsequently, by utilizing existing concave/convex optimization tools [27]. Overall, an effective, efficient, and well-established methodology is to employ the Dinkelback's algorithm [28], [29].

## D. Followers' Energy Efficiency Optimization

After the UAV reports back to the users the optimal bandwidth splitting ratio, the users' decision-making process takes place. Specifically, each user aims to distributively maximize its personal energy efficiency achieved at the access network part, by optimizing its uplink transmission power to the UAV. Hence, each user's *n* personal utility function is expressed as:

$$EE_n(P_n, \mathbf{P}_{-n}) = \frac{R_n^{AC}}{P_n},\tag{26}$$

where  $\mathbf{P}_{-n} = [P_1, \dots, P_{n-1}, P_{n+1}, \dots, P_{|N|}]$  is the vector of uplink transmission powers of all users except for user n. The interactions among the users are captured via a non-cooperative game  $G = [N, \{A_n\}_{\forall n \in N}, \{EE_n\}_{\forall n \in N}]$ , where N is the set of players, i.e., the users,  $A_n = [0, P_n^{max}]$  is each user's strategy set, i.e., the set of feasible uplink transmission power levels, as indicated by the user's maximum power budget  $P_n^{max}$ , and  $EE_n$  is each user's payoff function, i.e., its energy efficiency. The non-cooperative game G is treated as a distributed utility maximization problem, in which each user n updates its uplink transmission power  $P_n$  selfishly, by having prior information about the rest of the users' transmission powers  $\mathbf{P}_{-n}$  as broadcasted by the UAV, seeking to maximize its perceived satisfaction, i.e., its energy efficiency. The corresponding optimization problem that is solved by each user is

formulated as:

$$\max_{P_n} EE_n(P_n, \mathbf{P}_{-n}) = \frac{R_n^{AC}}{P_n}, \ \forall n \in \mathbb{N}$$
s.t.  $P_n \leq P_n^{max}, \ \forall n \in \mathbb{N}$  (27a)

s.t. 
$$P_n \le P_n^{max}, \ \forall n \in N$$
 (27b)

$$G_n P_n - \sum_{n'=1}^{n-1} G_{n'} P_{n'} \ge P_{tol}, n = 2, \dots, |N|$$
 (27c)

$$R_n^{AC} \ge R_{min}, \ \forall n \in N.$$
 (27d)

Apart from the maximum power budget constraint that the user's uplink transmission power to the UAV should meet, as imposed by Eq. (27b), Eq. (27c)-(27d) denote the extra group of constraints that the users' n strategy  $P_n$  should satisfy. Eq. (27c) guarantees that the SIC technique is successfully performed at the UAV's receiver, according to the receiver's sensitivity/tolerance  $P_{tol}$ , while Eq. (27d) ensures the user's minimum acceptable data rate QoS requirement  $R_{min}$ .

Let us denote as  $\Gamma_n$  the strategy space of each user, formed by the inclusion of the extra set of constraints in Eq. (27c)-(27d), i.e.,  $\Gamma_n = \{(P_n) \text{ satisfies Eq. (27c)-(27d)}\}.$ Then, each user's n overall feasible strategy space is reformulated as  $\Delta_n = A_n \cap \Gamma_n, \forall n \in N$  and the non-cooperative game is restructured as  $G = [N, \{\Delta_n\}_{\forall n \in \mathbb{N}}, \{EE_n\}_{\forall n \in \mathbb{N}}].$ 

Towards solving the updated non-cooperative game G, the widely used concept of Nash equilibrium is adopted. The Nash equilibrium point is the users' strategy vector  $\mathbf{P}^*$  =  $[P_1,\ldots,P_n,\ldots,P_{|N|}]$ , from which no user has the incentive to deviate, given the strategies of the rest of the users. The interested readers can refer to [30] for a more detailed definition and description of the Nash equilibrium concept.

To further accommodate our discussion regarding the existence of at least one Nash equilibrium point for the noncooperative game G and thus, the convergence of the users' strategies to the Nash equilibrium, we adopt the theory of the n-person generalized concave games [31].

Theorem 1 (Existence of Nash Equilibrium): The noncooperative game G is a n-person generalized concave game and admits at least one Nash equilibrium point, if the following conditions hold true [31]:

- 1) the strategy sets  $\Delta_1, \ldots, \Delta_{|N|}$  are non-empty, compact, convex subsets of finite dimensional Euclidean spaces,
- 2) all payoff functions  $EE_1, \ldots, EE_{|N|}$  are continuous on  $\Delta = \Delta_1 \times \cdots \times \Delta_{|N|},$
- 3) every payoff  $EE_n$  is a quasi-concave function of  $P_n$ over  $\Delta_n$  if all the other strategies are held fixed.

*Proof:* The Theorem 1 is proved by exploiting the content of Lemmas 1-2 introduced in III-C, properly adapted to suit to the energy efficiency function in Eq. (27a) and the constraints defined in Eq. (27b)-(27d). Condition 1 of Theorem 1 holds true following a similar procedure to Lemma 2. Condition 2 holds true given that the energy efficiency function is continuous on the users' strategy space  $\Delta$ . Last, condition 3 holds true following the analysis presented in Lemma 1, verifying that the energy efficiency function in Eq. (27a) is strictly quasiconcave. Therefore, the non-cooperative game G is a n-person generalized concave game and at least one Nash equilibrium point exists.

The convergence of the users' strategies to the Nash equilibrium point is achieved by implementing a Best Response Dynamics algorithm [32], as shown in Algorithm 1. At each iteration of the Best Response Dynamics algorithm, the quasiconcave optimization problem defined in Eq. (27a)-(27d) for each user is equivalently transformed and treated as a series of convex optimization problems via the Dinkelbach's algorithm, following the procedure described earlier in Section III-C.

## E. Stackelberg Game-Based Optimization Process

After the convergence of the users' strategies, their optimal uplink transmission powers P\*, are fed back to the UAV to establish the next iteration of the Stackelberg game. In other words, the optimization problem in Eq. (21a)-(21d) and the non-cooperative game among the users are iteratively solved and the output of the one acts as input to the other, complying to the relationship between the leader and the followers. This iterative procedure results to the Stackelberg equilibrium  $(\mu^*, P_U^*, \mathbf{P}^*)$  that concludes the preceding mathematical analysis in Sections III-C and III-D.

The complete Stackelberg game-based optimization process and operation of the proposed dynamic resource management framework is summarized in Algorithm 1. Note that the superscript (i) is used to dictate the value of each variable after the *i*-th iteration of the leader's and followers' optimization stages, which are iteratively updated until convergence is reached, whereas the superscript (j) is used to indicate the iterations required for the nested non-cooperative game that is played among the users.

To calculate the computational complexity of the Stackelberg game-based optimization process presented in Algorithm 1, the following algorithmic complexities should be first considered alone. The complexity of the optimization problem in Eq. (20a)-(20c) can be regarded as  $\mathcal{O}(M^x)$ , where  $1 \le x \le 4$ , by employing an interior-point algorithm intended for linear programming [33]. The sorting of the users according to their channel power gain can be performed with complexity  $\mathcal{O}(N^2)$  via the well-known Quicksort algorithm [34], while the search within the set S is of  $\mathcal{O}(\log(K))$ complexity when using the Binary Search algorithm [34], where K denotes the number of bandwidth splitting ratio values tested (i.e., K = 19). Concerning the Dinkelbach's algorithm, it is known to have a super-linear convergence rate [28], [29], while the asymptotic complexity of each convex optimization problem addressed at each iteration of the Dinkelbach's algorithm is polynomial in the number of optimization variables [17], [35]. Hence, our resulting single-variable problems have computational complexity equal to  $\mathcal{O}(1)$ . The remainder of the typical mathematical manipulations are of  $\mathcal{O}(1)$  complexity and are omitted, while we also assume that the distributed non-cooperative game among the users is performed in parallel.

For representation purposes and following commonly used methodologies, let  $I_D^U$  and  $I_D^n$  denote the number of Dinkelbach's algorithm's iterations required to solve the UAV's and each user's n optimization problems in Eq. (21a)-(21d) and Eq. (27a)-(27d), respectively. Also, we

# Algorithm 1 Stackelberg Game-Based Optimization Process

```
1: Initialize network simulation topology, including users',
    RIS's, UAV's and mBS's locations.
2: Initialize \psi, \beta, \eta_{LoS}, \eta_{NLoS}, f_c, c, a_U, \rho, a_R, d_s, W, N_0,
    P_U^{max}, P_n^{max}, P_{tol}, R_{min}.
3: Determine RIS elements' phase-shift adaptation by solv-
    ing Eq. (20a)-(20c) and calculate G_n, \forall n \in \mathbb{N}.
 4: Sort users in ascending order according to G_n.
 5: Initialize randomly P_U \in [0, P_U^{max}].
6: Set i = 0.
7: repeat
       Set i = i + 1.
8:
       for \mu = 0.05 : 0.05 : 0.95 do
 9:
10:
         Determine optimal uplink transmission power P_{II}^* by
          solving Eq. (21a)-(21d) with respect to P_U.
11:
          Add solution \{(\mu, P_{II}^*), EE_{II}^*\} to \mathcal{S}.
12:
       Select \{(\mu^*, P_U^*), EE_U^*\} from S, for which EE_U^* is the
13:
```

```
maximum in \mathcal{S}.

Set \mu^{*(i)} = \mu^* and P_U^{*(i)} = P_U^*.

Initialize randomly P_n \in \Delta_n, \ \forall n \in N.
14:
15:
```

Set j = 0. 16:

repeat 17: Set j = j + 1. 18:

for  $n \in N$  do 19:

Determine optimal uplink transmission power 20:  $P_n^{*(j)}$  by solving Eq. (27a)-(27d).

21: **end for**22: **until**  $|P_n^{*(j)} - P_n^{*(j-1)}| \le \epsilon, \forall n \in \mathbb{N}$ , where  $\epsilon \approx 10^{-5}$ .
23: **until**  $|P_U^{*(i)} - P_U^{*(i-1)}| \le \epsilon$ , where  $\epsilon \approx 10^{-5}$ .

indicate as I and J the total number of iterations required for the Stackelberg and the nested non-cooperative game to converge, accordingly. Consequently, the overall computational complexity of Algorithm 1 is equal to  $\mathcal{O}(M^x + N^2 + I \cdot (K \cdot I))$  $I_D^U \cdot 1 + log(K) + J \cdot I_D^n \cdot 1$ ). Indicative numerical results regarding the actual number of required Stackelberg game iterations, as well as the real execution time needed to converge to the Stackelberg equilibrium, are presented in Section V below.

## IV. END-TO-END DATA RATE OPTIMIZATION

In this section, we extend our proposed dynamic spectrum and power management framework, analyzed in detail in Section III, to account for an alternative objective, namely the end-to-end data rate optimization. On the one hand, we aim to corroborate on the reconfigurability and adaptability of the devised resource optimization framework, under different optimization objectives, while revealing the benefits introduced by the proper manipulation of the wireless propagation environment alongside. On the other hand, we seek to macroscopically identify and promote the significance of energy efficiency optimization.

Specifically, with reference to the resource optimization framework design presented in Section III, we subsequently introduce its counterpart towards maximizing the IAB network's end-to-end data rate. The joint optimization problem is formulated and solved in a distributed manner, following once again the principles of the Stackelberg games. Next, the three-stage optimization procedure adopted and explained in Fig. 2 is presented in a concise, though comprehensive manner, emphasizing on the main differences arising from the different optimization objective.

In accordance to the methodology followed in Section III, the first stage of the dynamic resource management framework towards the end-to-end data rate optimization, refers to the appropriate RIS elements' phase-shift adaptation by the UAV, which concludes to its increased received signal strength. The RIS elements' adaptation is performed following the proposed intelligent and of low-complexity approach described in Section III-B. Then, the second stage takes place and the UAV proceeds to the derivation of the optimal bandwidth splitting ratio and its personal transmission power to the mBS, which maximize the sum users' end-to-end data rate, given the users' uplink transmission powers. The corresponding optimization problem solved by the UAV is written as:

$$\max_{\mu, P_U} \sum_{n=1}^{|N|} R_n^{E2E} \tag{28a}$$

s.t. 
$$0 \le \mu \le 1$$
 (28b)

$$P_U \le P_U^{max} \tag{28c}$$

$$P_U \le P_U^{max}$$
 (28c)  
 $R_n^{E2E} \ge R_{min}, \quad \forall n \in N,$  (28d)

where the constraints in Eq. (28b)-(28d) are in accordance with the ones introduced in the energy efficiency optimization problem counterpart. The problem defined in Eq. (28a)-(28d) is, once again, solved with respect to  $P_U$  under a range of values of the parameter  $\mu$ , as discussed in Section III-C. Thus, we derive the optimal solution  $(\mu^*, P_U^*)$ .

In the third stage, the users optimize in an autonomous and distributed manner their uplink transmission powers to the UAV, such that their personal data rate in the access network part is maximized. The optimization problem to be solved by each user is given by:

$$\max_{P_n} R_n^{AC}(P_n, \mathbf{P}_{-n}), \ \forall n \in N$$
 (29a)

s.t. 
$$P_n \le P_n^{max}, \ \forall n \in \mathbb{N}$$
 (29b)

$$G_n P_n - \sum_{n'=1}^{n-1} G_{n'} P_{n'} \ge P_{tol}, \ n = 2, \dots, |N|$$
 (29c)

$$R_n^{AC} \ge R_{min}, \ \forall n \in N.$$
 (29d)

Once again, their in-between interactions are coordinated through a non-cooperative game, according to which each user n updates its uplink transmission power (i.e., its strategy) in a selfish way, given the other users' strategies  $P_{-n}$ . The outcome of the non-cooperative game is the Nash equilibrium point of the users' strategies, i.e., the vector  $P^*$  $[P_1,\ldots,P_n,\ldots,P_{|N|}]$ . The analysis, based on which the existence of at least one Nash equilibrium and the convergence at this point is ensured, follows the n-person concave games due to the objective function's strict concavity on  $P_n$ ,  $\forall n \in N$ and is analogous to the one incorporated in Section III-D. The second and third optimization stages are iteratively performed

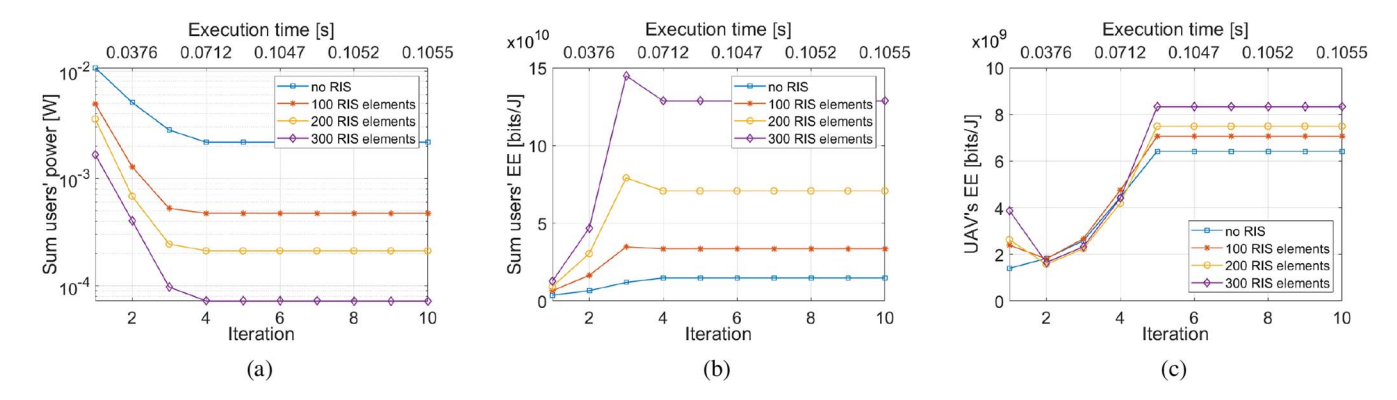


Fig. 3. Evaluation of the performance and the convergence behavior of the Stackelberg game-based process towards the end-to-end energy efficiency optimization, under different number of RIS elements.

and updated between the UAV and the users to ultimately conclude to the overall system's Stackelberg equilibrium point  $(\mu^*, P_U^*, \mathbf{P}^*)$ , as illustrated in Fig. 2.

## V. EVALUATION & RESULTS

In this section, we evaluate the performance and effectiveness of the proposed end-to-end resource management framework, via modeling and simulation. First, the pure performance of the distributed Stackelberg game, as well as its convergence behavior to the Stackelberg equilibrium is demonstrated, targeting the energy efficiency of the considered IAB network. Then, a comparative analysis between the two distinct optimization objectives tackled in this paper, namely the end-to-end energy efficiency optimization analyzed in Section III and the end-to-end data rate optimization approach summarized in Section IV, is enclosed. Finally, our proposed resource management framework is compared against different baseline resource management approaches in terms of both the RIS elements' phase shifts adaptation and the dynamic spectrum management solutions devised in this paper.

The simulation setting used to generate the numerical results presented in the remainder of this section is initialized as follows. Considering a three-dimensional coordinates system, the three main network entities of the RIS-aided and UAVassisted IAB network, i.e., the RIS, the UAV and the mBS, are located along the y = x line and their distances from the coordinates system's origin are set to 100 m, 200 m, and 400 m, respectively. The UAV hovers at 150 m above the ground, whereas the RIS, composed by |M| = 100 elements (unless mentioned otherwise), is placed at a height of 1.5 m and in close proximity to the users. We consider a NOMA cluster of |N| = 4 users in total, placed with increasing distances from the RIS, denoted as  $d_1$  [m],  $d_1 + 10$  [m],  $d_1 + 20$  [m],  $d_1 + 30$  [m], respectively, where  $d_1$  indicates the distance of the first user from the RIS and is generally set as  $d_1 = 5$  m unless otherwise stated. The parameters that characterize the wireless propagation environment are configured as:  $\psi = 11.95$ ,  $\beta = 0.14$ ,  $\eta_{LoS} = 3$  dB,  $\eta_{NLoS} = 23$  dB,  $f_c = 2 \text{ GHz}, c = 3 \cdot 10^8 \text{ m/s}, a_U = 2, \rho = 100, a_R = 2.8,$  $d_s = \frac{\lambda}{2}$ . The remaining communications-related simulation parameters are set as: W = 5 MHz,  $N_0 = -174$  dBm/Hz,  $P_n^{max} = 24 \text{ dBm}, P_{II}^{max} = 46 \text{ dBm}, P_{tol} = -114 \text{ dBm},$ 

 $R_{min} = 1$  Mbps, unless otherwise explicitly stated. Finally, for statistical purposes, the results have been averaged over 100 different channel model realizations.

1) Pure Evaluation of the Stackelberg Game-Based Optimization Process: In Fig. 3, we study the performance of the overall Stackelberg game-based process towards the IAB network's energy efficiency optimization, while at the same time assessing its convergence behavior with respect to the number of iterations I and the real execution time required to converge to the Stackelberg equilibrium point. Specifically, Fig. 3(a) depicts the sum users' uplink transmission powers as a function of the required iterations and the real execution time in seconds. The different curves present an analysis over a different number of RIS elements |M| = [100, 200, 300],while the term "no RIS" refers to the case where no RIS exists within the simulated network topology. The real execution time has been calculated as the mean execution time of the four different RIS elements' scenarios, as presented above. On the one hand, the results reveal that after a small number of iterations (e.g., I = 5 iterations or approximately 0.085 seconds in the case under consideration) the proposed approach converges to the optimal solution. On the other hand, it is confirmed that the use of RIS concludes to significantly lower power levels for the users, owing to the increased channel power gains incurred by the proper adaptation of the RIS elements' phase shifts. Given that the optimization objective targeted is the network's energy efficiency, the decreased sum users' power levels leads apparently to the remarkable increase of the sum users' energy efficiency, as illustrated in Fig. 3(b). The findings of Fig. 3(b) demonstrate that the use of RIS can provide almost 1.5 orders of magnitude higher sum users' energy efficiency, considering a number of |M| = 300RIS elements, compared to the case where no RIS exists in the network topology. Although the RIS is deployed in the access network part, directly affecting the users' power and energy efficiency, it results in the end-to-end system's optimized performance, as indicated in Fig. 3(c). Fig. 3(c) shows the pure UAV's energy efficiency, which is calculated as the fraction of the UAV's achieved data rate at the backhaul to its consumed uplink transmission power. Apparently, the access network's optimized performance steers the end-toend system's Stackelberg equilibrium to more energy-efficient points. Furthermore, the introduction of a RIS deployed at a

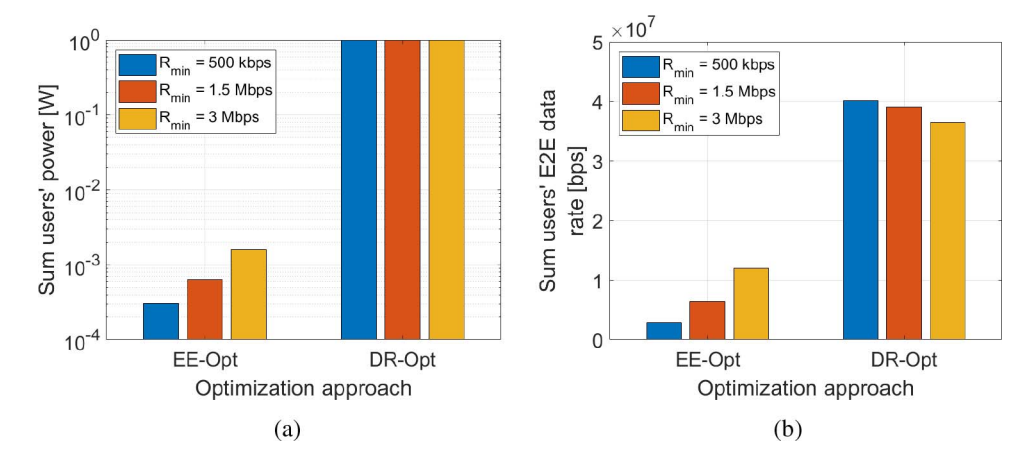


Fig. 4. Comparative evaluation between the two distinct end-to-end energy efficiency and data rate optimization approaches, under different users' minimum end-to-end data rate requirements.

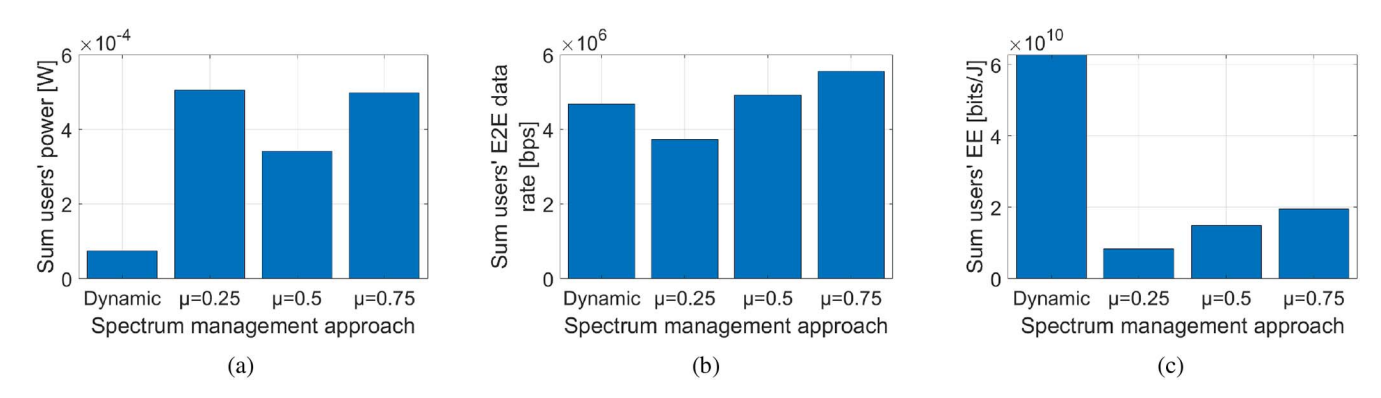


Fig. 5. Comparative evaluation of the proposed dynamically allocated spectrum solution between the access and backhaul network parts, against different fixed bandwidth splitting approaches.

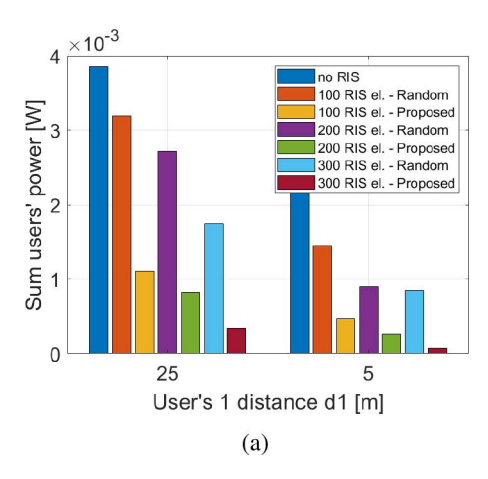
higher point above the ground and in LoS with the UAV, can further enhance the UAV's performance and strengthen the communications established at the backhaul network part.

Evaluation Different 2) Comparative of Network Optimization Objectives: To gain more insight regarding the significance of energy efficiency optimization objective in the wireless network's performance, we proceed to a comparative examination between the two distinct optimization objectives of end-to-end energy efficiency and end-to-end data rate maximization tackled in the paper. In particular, in Fig. 4 we scrutinize network's performance in terms of the sum users' transmission power levels and their achieved sum end-to-end data rates under the two different optimization objectives/approaches, which are denoted as "EE-Opt" and "DR-Opt". Furthermore, a study over different values  $R_{min} = [0.5, 1.5, 3]$  Mbps of the users' minimum end-to-end data rate requirement accompanies our analysis, to further identify and highlight the network's enhanced performance under the energy efficiency optimization approach, considering different user QoS requirements.

Apparently, when the "DR-Opt" optimization approach is treated, the users are forced to transmit in the uplink using their maximum power budget regardless of their minimum data rate QoS requirement  $R_{min}$ , as properly presented in Fig. 4(a). On the contrary, the sum users' transmission powers are approximately thirty times lower in the case of "EE-Opt" compared to "DR-Opt", while a slight increase is imposed as

the minimum data rate requirement increases. The sum users' end-to-end data rates achieved by utilizing the sum power levels of Fig. 4(a), are accordingly shown in Fig. 4(b). It can be easily observed that the thirty-times increase in the users' power levels results in almost only three orders higher end-to-end data rates, verifying the significant gains provided by the "EE-Opt", mainly in terms of the resulting efficiency. Last, it should be noted that the small decrease in the sum users' end-to-end data rates, induced as the  $R_{min}$  requirement increases, is due to need for higher bandwidth portion in the access network part that is shared among the users which are interfering with each other, such that the remaining bandwidth part pertaining to the backhaul network part decreases.

3) Evaluation of the Dynamic Spectrum Management: Subsequently, we aim to investigate the effectiveness and efficiency of the proposed end-to-end resource management framework with regards to the dynamically allocated spectrum in the access and backhaul network parts, under our primarily targeted energy efficiency optimization objective. Towards this direction, our dynamic spectrum management solution is compared against other heuristic mechanisms that assume a fixed bandwidth partitioning between the two network parts (i.e., access and backhaul). For demonstration purposes, three different fixed bandwidth splitting schemes are considered with bandwidth splitting ratio parameter values equal to  $\mu = [0.25, 0.5, 0.75]$ . The outcome of this comparison is presented in Fig. 5, where the term "Dynamic" refers to



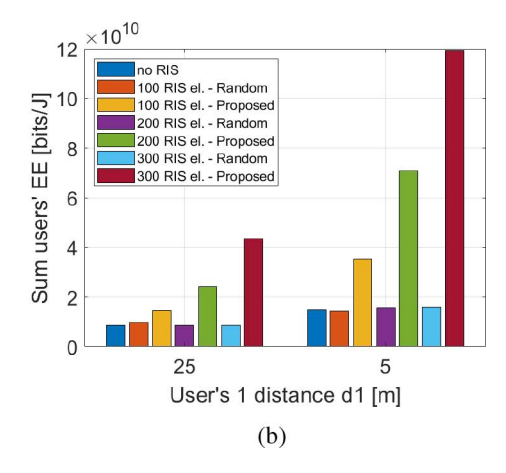


Fig. 6. Comparative evaluation of the proposed RIS elements' phase-shift adaptation method against a random phase-shift configuration approach, under different number of RIS elements and distances of the users from the RIS.

our proposed dynamically allocated spectrum procedure. The numerical results in Fig. 5 have been specifically averaged over 300 different IAB network topologies, considering different locations of the mBS, which range from 400 m to 700 m far form the origin of the three dimensional coordinates system, to account for the potential different needs in terms of bandwidth splitting among the access and backhaul network parts. Evidently, the proposed dynamic spectrum management solution results in remarkably lower sum users' power levels compared to any of the fixed bandwidth splitting schemes, as demonstrated in Fig. 5(a). Moreover, a small only differentiation occurs in the achieved sum users' endto-end data rates under the different spectrum management approaches (Fig. 5(b)). Nevertheless, the dominance of the dynamically allocated spectrum is clearly identified, when considering the sum users' energy efficiency achieved, as presented in Fig. 5(c).

4) Evaluation of the Proposed RIS Elements' Phase-Shift Adaptation: Our evaluation analysis is complemented with an extensive study pertinent to the performance gain provided by the introduction of the RIS within the network topology, as well as its proper configuration and phase-shift adaptation via our proposed method, as described in Section III-B. To this end, we compare our proposed RIS elements' phaseshift adaptation method against a baseline approach, in which a random phase shift configuration is selected for the RIS, referred to as "Random" in the following. In Fig. 6, appropriate results corresponding to the two different phase-shift configuration schemes, i.e., the "Proposed" one and the "Random" one, are extracted considering different number of RIS elements |M| = [100, 200, 300] and different distances of the users' from the RIS. The different users' distance scenarios from the RIS are indicated via the first user's distance  $d_1$  [m] from the RIS along the x axis. Also, the general case where no RIS exists within the network simulated topology is included as a reference scenario. In particular, in Fig. 6(a), the sum users' power levels are depicted as a function of the different phase-shift configuration schemes and the different users' distances. Apparently, as the number of RIS elements increases, the sum users' uplink transmission powers

decrease, resulting correspondingly to their increased sum achieved energy efficiency, as indicated by Fig. 6(b).

#### VI. CONCLUSION & FUTURE WORK

Several technologies have recently emerged that shape the frontier of the future wireless networks' era, prospective candidates of which constitute the network deployment paradigm of Integrated Access and Backhaul (IAB) and the Reconfigurable Intelligent Surafce (RIS). In this paper, we identify the potentials brought by their joint inclusion in the future wireless networks' environment, through the introduction of a converged RIS-aided and UAV-assisted IAB network, while targeting to ameliorate the overall network's energy efficiency along the wireless access and backhaul network parts. To this end, we devise an end-to-end resource management framework, primarily founded on the concepts of reconfigurability and adaptability, to account for and appropriately control the RIS elements' phase shifts, the bandwidth splitting between the wireless access and backhaul, and the transmission powers of both the users and the UAV. To efficiently treat the joint optimization problem, we propose a distributed optimization process based on the Stackelberg games, according to which the network resources are allocated in different stages. Extensive numerical results highlight the benefits and performance gains derived from the operation of the dynamic resource management of the RIS-aided and UAV-assisted IAB network.

Part of our current and future work refers to the inclusion of multiple UAVs and RISs within the network topology, implying the need for intelligent resource management solutions that consider the increased network's degrees of freedom and complexity, while accounting for the UAVs' and the users' mobility. Other research extensions include the utilization of the RIS as a network entity that facilitates the proactive handover management of the users' data traffic, instead of simply used to optimize different network-specific metrics. Finally, the challenge of identifying the lower and upper bounds for the optimal RIS elements' phase shifts adaptation, constitutes another major, though unsolved, problem in the current

literature that needs to be addressed in order to reap the benefits of the RIS, and exploit it at its full potential.

#### REFERENCES

- C. Madapatha *et al.*, "On integrated access and backhaul networks: Current status and potentials," *IEEE Open J. Commun. Soc.*, vol. 1, pp. 1374–1389, 2020.
- [2] Technical Specification Group Radio Access Network; NR; Study on Integrated Access and Backhaul; (Release 16), Version 16.0.0., 3GPP Standard (TS) 38.874, Dec. 2018,
- [3] S. Gong et al., "Toward smart wireless communications via intelligent reflecting surfaces: A contemporary survey," *IEEE Commun. Surveys Tuts.*, vol. 22, no. 4, pp. 2283–2314, 4th Quart., 2020.
- [4] X. Pei et al., "RIS-aided wireless communications: Prototyping, adaptive beamforming, and indoor/outdoor field trials," 2021, arXiv:2103.00534.
- [5] J. Y. Lai, W.-H. Wu, and Y. T. Su, "Resource allocation and node placement in multi-hop heterogeneous integrated-access-and-backhaul networks," *IEEE Access*, vol. 8, pp. 122937–122958, 2020.
- [6] W. Lei, Y. Ye, and M. Xiao, "Deep reinforcement learning-based spectrum allocation in integrated access and backhaul networks," *IEEE Trans. Cogn. Commun. Netw.*, vol. 6, no. 3, pp. 970–979, Sep. 2020.
- [7] Q. Zhang, W. Ma, Z. Feng, and Z. Han, "Backhaul-capacity-aware interference mitigation framework in 6G cellular Internet of Things," *IEEE Internet Things J.*, vol. 8, no. 12, pp. 10071–10084, Jun. 2021.
- [8] N. Tafintsev et al., "Aerial access and backhaul in mmWave B5G systems: Performance dynamics and optimization," *IEEE Commun. Mag.*, vol. 58, no. 2, pp. 93–99, Feb. 2020.
- [9] M.-J. Youssef, J. Farah, C. A. Nour, and C. Douillard, "Full-duplex and backhaul-constrained UAV-enabled networks using NOMA," *IEEE Trans. Veh. Technol.*, vol. 69, no. 9, pp. 9667–9681, Sep. 2020.
- [10] L. Zhang and N. Ansari, "Optimizing the deployment and throughput of DBSs for uplink communications," *IEEE Open J. Veh. Technol.*, vol. 1, pp. 18–28, Nov. 2020.
- [11] A. Fouda, A. S. Ibrahim, Í. Güvenç, and M. Ghosh, "Interference management in UAV-assisted integrated access and backhaul cellular networks," *IEEE Access*, vol. 7, pp. 104553–104566, 2019.
- [12] B. Zheng, Q. Wu, and R. Zhang, "Intelligent reflecting surface-assisted multiple access with user pairing: NOMA or OMA?" *IEEE Commun. Lett.*, vol. 24, no. 4, pp. 753–757, Apr. 2020.
- [13] Y. Guo, Z. Qin, Y. Liu, and N. Al-Dhahir, "Intelligent reflecting surface assisted NOMA over fading channels," in *Proc. IEEE Global Commun. Conf. (GLOBECOM)*, Taipei, Taiwan, 2020, pp. 1–6.
- [14] X. Gao, Y. Liu, X. Liu, and Z. Qin, "Resource allocation in IRSs aided MISO-NOMA networks: A machine learning approach," in *Proc. IEEE Global Commun. Conf. (GLOBECOM)*, Taipei, Taiwan, 2020, pp. 1–6.
- [15] M. Zeng, X. Li, G. Li, W. Hao, and O. A. Dobre, "Sum rate maximization for IRS-assisted uplink NOMA," *IEEE Commun. Lett.*, vol. 25, no. 1, pp. 234–238, Jan. 2021.
- [16] Y. Cheng, K. H. Li, Y. Liu, K. C. Teh, and H. V. Poor, "Downlink and uplink intelligent reflecting surface aided networks: NOMA and OMA," *IEEE Trans. Wireless Commun.*, vol. 20, no. 6, pp. 3988–4000, Jun. 2021.
- [17] J. Xiong, L. You, D. W. K. Ng, C. Yuen, W. Wang, and X. Gao, "Energy efficiency and spectral efficiency tradeoff in RIS-aided multiuser MIMO uplink systems," in *Proc. IEEE Global Commun. Conf. (GLOBECOM)*, Taipei, Taiwan, 2020, pp. 1–6.
- [18] Z. Wei, Y. Cai, Z. Sun, D. W. K. Ng, and J. Yuan, "Sum-rate maximization for IRS-assisted UAV OFDMA communication systems," in *Proc. IEEE Global Commun. Conf. (GLOBECOM)*, 2020, pp. 1–7.
- [19] X. Liu, Y. Liu, and Y. Chen, "Machine learning empowered trajectory and passive beamforming design in UAV-RIS wireless networks," *IEEE J. Sel. Areas Commun.*, vol. 39, no. 7, pp. 2042–2055, Jul. 2021.
- [20] Q. Zhang, W. Saad, and M. Bennis, "Distributional reinforcement learning for mmWave communications with intelligent reflectors on a UAV," in *Proc. IEEE Global Commun. Conf. (GLOBECOM)*, Taipei, Taiwan, 2020, pp. 1–6.
- [21] Q. Wu and R. Zhang, "Intelligent reflecting surface enhanced wireless network via joint active and passive beamforming," *IEEE Trans. Wireless Commun.*, vol. 18, no. 11, pp. 5394–5409, Nov. 2019.
- [22] S. Jia, X. Yuan, and Y.-C. Liang, "Reconfigurable intelligent surfaces for energy efficiency in D2D communication network," *IEEE Wireless Commun. Lett.*, vol. 10, no. 3, pp. 683–687, Mar. 2021.

- [23] S. Li, B. Duo, X. Yuan, Y.-C. Liang, and M. Di Renzo, "Reconfigurable intelligent surface assisted UAV communication: Joint trajectory design and passive beamforming," *IEEE Wireless Commun. Lett.*, vol. 9, no. 5, pp. 716–720, May 2020.
- [24] P. D. Diamantoulakis, K. N. Pappi, and G. K. Karagiannidis, "Jointly optimal downlink/uplink design for wireless powered networks," in *Proc.* 24th Int. Conf. Telecommun. (ICT), 2017, pp. 1–6.
- [25] S. Boyd and L. Vandenberghe, Convex Optimization. Cambridge, U.K.: Cambridge Univ. Press, 2004.
- [26] S. Schaible, Fractional Programming. Boston, MA, USA: Springer, 2013.
- [27] T. Coleman, M. A. Branch, and A. Grace, Optimization Toolbox For Use with MATLAB: User's Guide, Version 2, MathWorks, Natick, MA, USA, 1990.
- [28] W. Dinkelbach, "On nonlinear fractional programming," Manage. Sci., vol. 13, no. 7, pp. 492–498, 1967. [Online]. Available: http://www.jstor.org/stable/2627691
- [29] A. Zappone and E. Jorswieck, "Energy efficiency in wireless networks via fractional programming theory," *Found. Trends Commun. Inf. Theory*, vol. 11, nos. 3–4, pp. 185–396, 2015.
- [30] E. E. Tsiropoulou, G. K. Katsinis, and S. Papavassiliou, "Distributed uplink power control in multiservice wireless networks via a game theoretic approach with convex pricing," *IEEE Trans. Parallel Distrib. Syst.*, vol. 23, no. 1, pp. 61–68, Jan. 2012.
- [31] F. Forgó, "On the existence of nash-equilibrium in n-person generalized concave game," in *Generalized Convexity* (Lecture Notes in Economics and Mathematical Systems), vol. 405, S. Komlósi, T. Rapcsák, and S. Schaible, Eds. Berlin, Germany: Springer, 1994.
- [32] E. E. Tsiropoulou, P. Vamvakas, G. K. Katsinis, and S. Papavassiliou, "Combined power and rate allocation in self-optimized multi-service two-tier femtocell networks," *Comput. Commun.*, vol. 72, pp. 38–48, Dec. 2015.
- [33] F. A. Potra and S. J. Wright, "Interior-point methods," J. Comput. Appl. Math., vol. 124, no. 1, pp. 281–302, 2000. [Online]. Available: https://www.sciencedirect.com/science/article/pii/S0377042700004337
- [34] T. H. Cormen, C. E. Leiserson, R. L. Rivest, and C. Stein, *Introduction to Algorithms*. Cambridge, MA, USA: MIT Press, 2009.
- [35] C. Huang, A. Zappone, G. C. Alexandropoulos, M. Debbah, and C. Yuen, "Reconfigurable intelligent surfaces for energy efficiency in wireless communication," *IEEE Trans. Wireless Commun.*, vol. 18, no. 8, pp. 4157–4170, Aug. 2019.



Maria Diamanti (Graduate Student Member, IEEE) received the Diploma degree in electrical and computer engineering from the Aristotle University of Thessaloniki in 2018. She is currently pursuing the Ph.D. degree and is a Research Assistant with the School of Electrical and Computer Engineering, National Technical University of Athens. Her research interests lie in the areas of 5G/6G wireless networks, resource management and optimization, contract theory, game theory, and reinforcement learning.



Panagiotis Charatsaris received the five-year Diploma degree from the School of Electrical and Computer Engineering, National Technical University of Athens. His diploma thesis focuses on the topic of Reconfigurable Intelligent Surfaces in Integrated Access and Backhaul Networks. His overall research interests lie in the broader area of resource optimization in 5G/6G wireless communications systems.



Eirini Eleni Tsiropoulou (Senior Member, IEEE) is currently an Assistant Professor with the Department of Electrical and Computer Engineering, University of New Mexico. Her main research interests lie in the area of cyber-physical social systems and wireless heterogeneous networks, with emphasis on network modeling and optimization, resource orchestration in interdependent systems, reinforcement learning, game theory, network economics, and Internet of Things. Five of her papers received the Best Paper Award at IEEE WCNC in 2012,

ADHOCNETS in 2015, IEEE/IFIP WMNC 2019, INFOCOM 2019 by the IEEE ComSoc Technical Committee on Communications Systems Integration and Modeling, and IEEE/ACM BRAINS 2020. She was selected by the IEEE Communication Society—N2Women—as one of the top ten Rising Stars of 2017 in the communications and networking field. She received the NSF CRII Award in 2019 and the Early Career Award by the IEEE Communications Society Internet Technical Committee in 2019.



Symeon Papavassiliou (Senior Member, IEEE) is currently a Professor with the School of ECE, National Technical University of Athens. From 1995 to 1999, he was a Senior Technical Staff Member with AT&T Laboratories, New Jersey. In August 1999, he joined the ECE Department, New Jersey Institute of Technology, USA, where he was an Associate Professor until 2004. He has an established record of publications in his field of expertise, with more than 300 technical journal and conference published papers. His main research interests lie in

the area of computer communication networks, with emphasis on the analysis, optimization, and performance evaluation of mobile and distributed systems, wireless networks, and complex systems. He received the Best Paper Award in IEEE INFOCOM 94, the AT&T Division Recognition and Achievement Award in 1997, the U.S. National Science Foundation Career Award in 2003, the Best Paper Award in IEEE WCNC 2012, the Excellence in Research Grant in Greece in 2012, the Best Paper Awards in ADHOCNETS 2015, ICT 2016 and IEEE/IFIP WMNC 2019, as well as the 2019 IEEE ComSoc Technical Committee on Communications Systems Integration and Modeling Best Paper Award (for his INFOCOM 2019 paper). He also served on the board of the Greek National Regulatory Authority on Telecommunications and Posts from 2006 to 2009.